

# Investigation of semicrystalline morphology in poly(ether ether ketone)/poly(ether imide) blends by dielectric relaxation spectroscopy

Joseph F. Bristow and Douglass S. Kalika\*

Department of Chemical and Material Engineering, University of Kentucky, Lexington, KY 40506-0046, USA

(Received 19 January 1996; revised 6 March 1996)

The semicrystalline morphology of a series of poly(ether ether ketone) [PEEK]/poly(ether imide) [PEI] blends has been investigated as a function of blend composition and crystallization condition by dielectric relaxation spectroscopy. Dielectric scans of the crystallized blends revealed two glass–rubber relaxations for all specimens corresponding to the coexistence of a mixed amorphous interlamellar phase, and a pure PEI phase residing in interfibrillar/interspherulitic regions; no (pure PEEK) crystal–amorphous interphase was observed. Variations in the composition of the mixed interlamellar phase with crystallization temperature were consistent with kinetic control of the evolving morphology: lower crystallization temperatures led to an increase in the amount of PEI trapped between crystal lamellae. Comparison of the relaxation characteristics of the interfibrillar/interspherulitic phase with those of pure PEI indicated a much broader spectrum of local relaxation environments for PEI in the blends, consistent with PEI segregation across a wide range of size scales. Copyright © 1996 Elsevier Science Ltd.

(Keywords: poly(ether ether ketone); poly(ether imide); crystallizable blends)

## INTRODUCTION

Blends of poly(ether ether ketone) [PEEK] with poly(ether imide) [PEI] represent a class of polymer blends of considerable commercial and academic interest, that is, miscible polymer blends containing a single crystallizable component. The elucidation of the morphology which develops upon crystallization of these blends is of interest not only in terms of the macroscopic product properties which are achieved as a function of blend composition and processing history, but also in terms of the additional insight which these systems provide as to the nature of noncrystalline regions in semicrystalline polymers in general. In the work reported here, dielectric relaxation spectroscopy has been used to investigate the segregation of PEI in thermally-crystallized PEEK/PEI blends as a function of blend composition and crystallization temperature. Dielectric spectroscopy affords a sensitive means by which to examine the dipolar mobilization characteristics of the amorphous phase populations in the vicinity of the glass–rubber relaxation. The measured relaxation temperatures and corresponding relaxation characteristics (i.e. relaxation intensity, breadth) provide information as to the composition and local morphological environment of the various amorphous constituents.

Poly(ether ether ketone) is a semicrystalline engineering thermoplastic which displays outstanding thermal and chemical resistance properties ( $T_g = 146^\circ\text{C}$ ;  $T_m \sim 340^\circ\text{C}$ ), while poly(ether imide) is an amorphous

engineering thermoplastic with a high glass transition temperature ( $T_g = 215^\circ\text{C}$ ). PEEK and PEI have been found to be fully miscible in the melt state, and upon quenching to an amorphous glass<sup>1,2</sup>. Calorimetric and dynamic mechanical/dielectric studies on quenched PEEK/PEI blends reveal a single glass transition, with the variation in  $T_g$  as a function of blend composition following the Fox equation<sup>1–5</sup>. PEEK/PEI blending leads to the enhancement of a number of physical properties of the blend relative to those of the individual components, including heat distortion temperature, solvent resistance, and overall toughness.

When PEEK/PEI blends are crystallized via annealing in the melt or rubbery state, the observed crystalline characteristics are largely unchanged relative to pure PEEK: the unit cell dimensions<sup>6</sup> and equilibrium melting temperature<sup>3</sup> remain the same (i.e. negligible melting point depression is observed), and the enthalpy of fusion varies approximately linearly with composition, indicating a nearly constant degree of crystallinity based on the PEEK fraction present in the blend<sup>1,2,4</sup>. As crystallization occurs, PEI is excluded from the evolving crystalline structures, and the amorphous regions are enriched in the noncrystallizable component. The morphology which results in the crystallized blend reflects the nature of the segmental interactions between the components, and the rate at which the PEI can diffuse away from the crystalline regions relative to the rate of crystallization. For systems with weak intersegmental interactions, rate effects typically govern the resultant morphology<sup>3</sup>.

\*To whom correspondence should be addressed

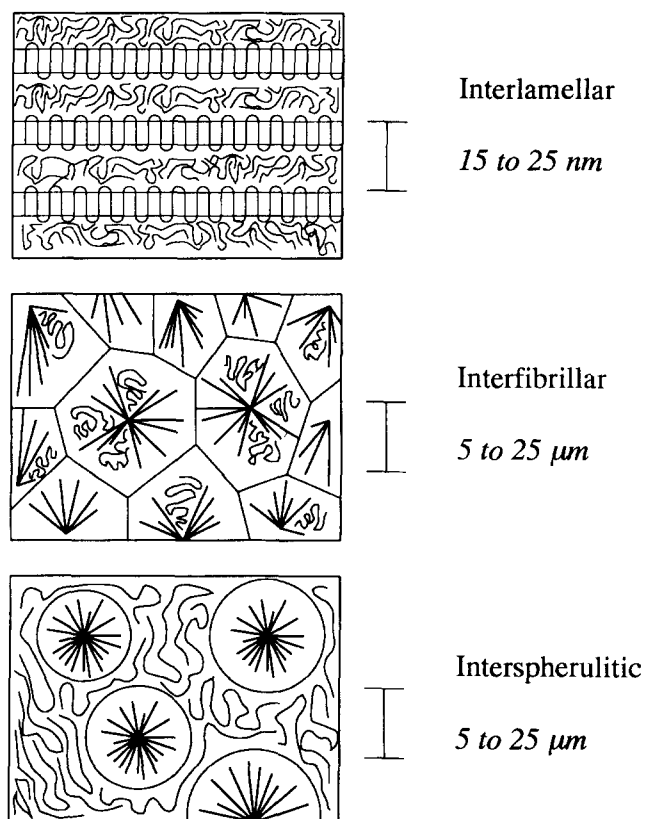


**Figure 1** Potential modes of PEI segregation in PEEK/PEI crystallized blends: interlamellar, interfibrillar, and interspherulitic (after Hsiao and Sauer<sup>3</sup>)

Three potential morphologies may be observed which reflect the nature of the PEI exclusion in crystallized PEEK/PEI blends: interlamellar, interfibrillar (inter-[lamellar-bundle]), and interspherulitic (Figure 1)<sup>2,3,6</sup>. For conditions at which the rate of crystallization is fast relative to the rate of PEI diffusion, the interlamellar morphology may dominate, while at conditions where the rate of crystallization is slow relative to the rate of PEI diffusion, interfibrillar or interspherulitic morphologies are favoured. In certain miscible blends containing crystallizable components of a flexible nature [e.g. poly(vinylidene fluoride)/poly(methyl methacrylate)<sup>7-9</sup>, poly(ethylene oxide)/poly(methyl methacrylate)<sup>10-11</sup>], a crystal-amorphous interphase region is observed at the lamellar surface from which the noncrystallizable component is completely excluded. This demixing of the crystallizable and noncrystallizable chains over a distance of approximately 2.0 nm reflects a persistence of order beyond the crystal surface which is consistent with theoretical lattice model calculations<sup>12,13</sup>. For blends containing crystallizable polymers of a somewhat stiffer nature, the pure crystal-amorphous interphase is not in evidence, suggesting penetration of the interphase region by the noncrystallizable chains<sup>14</sup>. Untransesterified blends of poly(butylene terephthalate) [PBT]/bisphenol A polyarylate [PAR] fall into this category. Dynamic mechanical and dielectric studies by Huo and Cebe<sup>15,16</sup> and Runt *et al.*<sup>17,18</sup> on PBT/PAR blends reveal two coexisting amorphous populations in the crystallized blend samples: a mixed amorphous phase, and a phase comprised of pure PAR. Small-angle X-ray scattering (SAXS) measurements indicate that interlamellar incorporation of the noncrystallizable PAR is favoured at

lower overall PAR content ( $<0.40$  weight fraction), while interfibrillar/interspherulitic segregation becomes important at higher PAR content ( $>0.40$ )<sup>16</sup>. The mixed phase corresponds to amorphous PBT and PAR chains located between crystal lamellae, while the pure PAR phase is the result of expulsion of the noncrystallizable component to interfibrillar and interspherulitic regions.

When semiflexible polymers such as PEEK are crystallized, the characteristics of the glass-rubber relaxation change significantly as compared to those of a wholly-amorphous (i.e. quenched) specimen. The presence of crystallinity results in a positive offset on order of 10–20°C in the glass transition temperature of the semicrystalline material as compared to its wholly-amorphous counterpart, as well as broadening of the glass transition<sup>19,20</sup>. These features reflect the considerable constraint imposed by the crystallites on the large-scale motions inherent to the glass transition, and indicate a fundamental difference between the amorphous portion of the semicrystalline PEEK chains and amorphous PEEK in the absence of crystallinity. In crystallizable polymer blends, the constraint imposed on the amorphous (crystallizable) chain segments by the crystal lamellae changes the nature of intersegmental interaction between the crystallizable and noncrystallizable components in the presence of crystallinity. For PEEK/PEI blends, this change is manifested in a significant degree of PEI segregation outside of the crystal lamellae into interfibrillar and interspherulitic regions. Electron and optical microscopy studies by Hudson *et al.*<sup>6</sup> clearly show the presence of PEI in interfibrillar regions across a wide range of crystallization temperatures, with interspherulitic segregation evident at the highest crystallization temperatures examined ( $>300^{\circ}\text{C}$ ). SAXS measurements by a number of investigators<sup>2-4</sup> reveal only a minimal dependence of long period/interlamellar spacing on blend composition, again consistent with expulsion of PEI to primarily interfibrillar/interspherulitic locations. Dielectric studies by Jonas *et al.*<sup>4</sup> indicate the coexistence of two amorphous populations: a mixed interlamellar phase, and a pure (interfibrillar/interspherulitic) PEI phase, similar to the results for PBT/PAR described above. A pure PEEK crystal-amorphous interphase region has not been observed for the PEEK/PEI blends.

In this paper, a comprehensive dielectric investigation of crystallized PEEK/PEI blends is reported. Specifically, dielectric relaxation spectroscopy is used to investigate the glass-rubber relaxation characteristics and corresponding amorphous phase separation in cold- and melt-crystallized PEEK/PEI blends as a function of blend composition and crystallization temperature. For all cases, two glass-rubber relaxations are observed corresponding to a mixed amorphous interlamellar phase, and a pure PEI phase residing in interfibrillar/interspherulitic regions; the relative fraction of PEI trapped in the interlamellar phase is increased at lower crystallization temperatures. Comparison of the relaxation characteristics of the interfibrillar/interspherulitic phase with those of pure PEI indicate that the PEI chains in the blend experience a broadened range of local relaxation environments, with the observed relaxation encompassing a spectrum of PEI segregation size-scales ranging from the interlamellar (nanometre scale) to the interfibrillar/interspherulitic (micrometre scale).

## EXPERIMENTAL

PEEK (Victrex 450G) was obtained in pellet form from Victrex U.S.A., Inc. PEI (Ultem 1000) was obtained through the courtesy of GE Plastics, Mount Vernon, IN. All materials were dried under vacuum prior to use. Blending of the resin pellets was accomplished by mechanical mixing followed by melt extrusion in a Custom Scientific Instruments (CSI) 194 mixing extruder at 370°C with pelletization of the resulting strands. Blend compositions of 75/25, 50/50, and 25/75 PEEK/PEI were prepared.

Blend films (~130  $\mu\text{m}$  thickness) for dielectric measurement were prepared by compression moulding in a Carver melt press at 400°C. Isothermally melt-crystallized samples were obtained by direct transfer of the films from the melt press to a second press held at the desired crystallization temperature. Melt crystallization temperatures were 280, 300, and 320°C. Crystallization times were 1 h for PEEK and the 75/25 and 50/50 PEEK/PEI compositions (280 and 300°C) and 3 h for the 25/75 blend; all crystallizations at 320°C were carried out for 3 h. Full crystallization of the samples was confirmed by isothermal calorimetric studies (see also refs 2 and 3).

Amorphous blend samples were obtained by quenching films from the melt (400°C) to an ice water bath; fully transparent films were obtained for PEEK and all blend compositions. Cold-crystallized samples were prepared by isothermal annealing of the quenched films in the press at the desired crystallization temperature; cold crystallization temperatures were 220, 240, 260, 280, and 300°C. Crystallization times were 1 h for 75/25 and 50/50 PEEK/PEI, 3 h for 25/75 PEEK/PEI. PEI films for dielectric measurements were prepared by compression moulding of the Ultem pellets at 300°C with cooling to ambient temperature. All sample films were vacuum dried at 50°C for at least 24 h prior to measurement.

Dielectric spectroscopy measurements were accomplished using a Polymer Laboratories dielectric thermal analyzer (PL-DETA) comprised of a GenRad Digi-bridge interfaced with the Polymer Laboratories temperature controller. Concentric silver electrodes (33 mm) were vacuum evaporated directly on the samples, which were mounted between polished platens in the temperature-controlled test oven; all measurements were carried out under an inert ( $\text{N}_2$ ) atmosphere. The dielectric constant ( $\epsilon'$ ) and loss factor ( $\tan \delta$ ) were recorded at frequencies ranging from 0.05 to 100 kHz across a temperature range from 50 to 300°C. The heating rate was 1.0°C min<sup>-1</sup> for PEEK and the blends, 0.75°C min<sup>-1</sup> for the pure PEI sample.

## RESULTS AND DISCUSSION

*Amorphous samples*

Dielectric results for a representative quenched amorphous blend sample (50/50 PEEK/PEI) are plotted isochronally as dielectric constant ( $\epsilon'$ ) and loss factor ( $\tan \delta$ ) vs. temperature in Figure 2. A strong increase in dielectric constant is observed starting at 160°C which corresponds to the onset of the glass-rubber relaxation in the single-phase amorphous sample; this is accompanied by a relatively sharp maximum in  $\tan \delta$ . The step-wise increase in  $\epsilon'$  characteristic of a dipolar relaxation is truncated

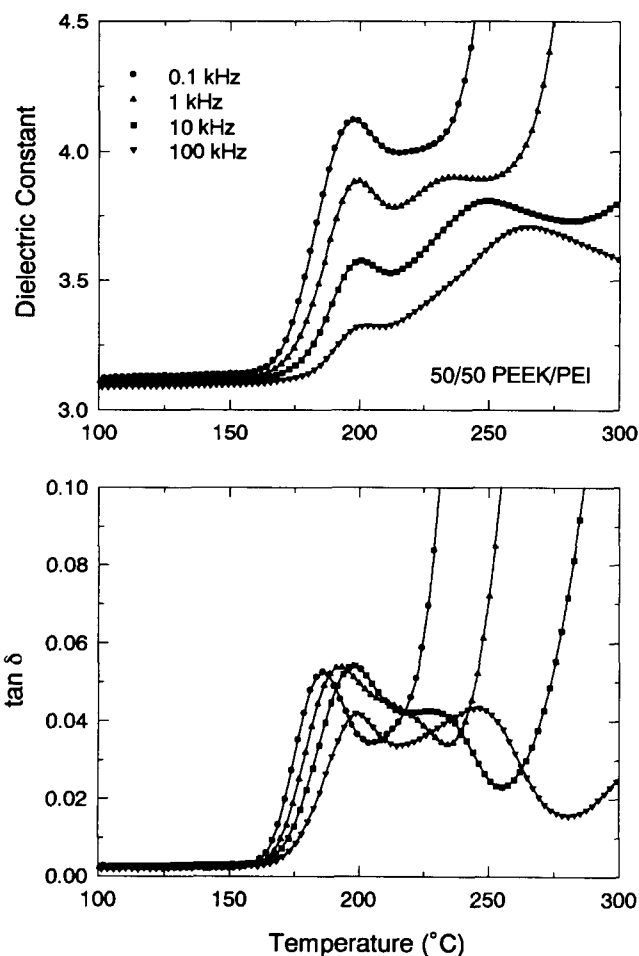


Figure 2 Dielectric constant ( $\epsilon'$ ) and loss factor ( $\tan \delta$ ) vs. temperature (°C) for quenched amorphous 50/50 PEEK/PEI blend. Frequencies of 0.1 (●), 1.0 (▲), 10 (■) and 100 (▼) kHz

by the onset of PEEK cold crystallization at ~200°C. Cold crystallization results in a decrease in the dielectric constant, and this is followed by a second apparent relaxation which corresponds to a complicated response owing to the mobilization of a constrained mixed phase located between crystal lamellae, as well as the relaxation of noncrystallizable chains excluded to interfibrillar/interspherulitic regions. The subsequent increase in dielectric constant and loss factor observed at lower test frequencies and higher temperatures reflects the onset of ionic conduction in the now multiphase sample.

A comparison of the glass-rubber relaxation results for the quenched blend specimens and their individual constituents is provided in Figure 3. Examination of the  $\tan \delta$  vs. temperature curves (1 kHz) reveals a systematic increase in relaxation temperature with increasing PEI content for these initially-amorphous samples. The glass-rubber relaxation is broadened in the blends as compared to the constituent homopolymers, with the influence of cold crystallization clearly evident on the high temperature side of the blend curves. Examination of the relaxation temperature as a function of PEI content (1 kHz test frequency, see Figure 4) shows good agreement with the Fox equation<sup>5</sup>. This is consistent with the calorimetric and dynamic studies cited above, and confirms the reported miscibility of this blend system.

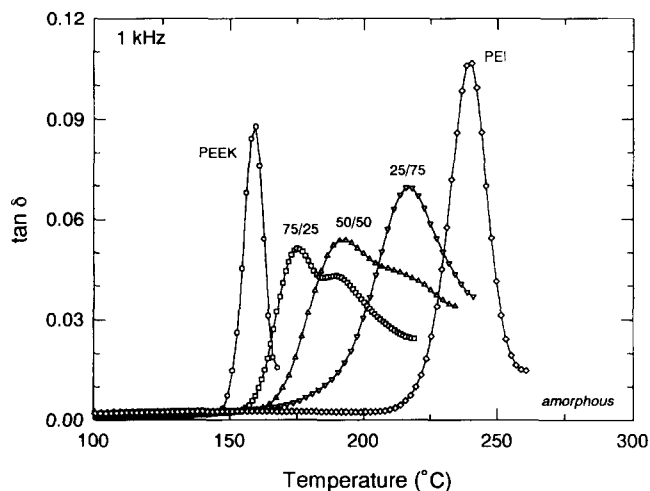


Figure 3 Dielectric  $\tan \delta$  (1 kHz) vs. temperature ( $^{\circ}\text{C}$ ) for amorphous PEEK/PEI blends of varying composition. PEEK ( $\circ$ ), 75/25 PEEK/PEI ( $\square$ ), 50/50 PEEK/PEI ( $\Delta$ ), 25/75 PEEK/PEI ( $\nabla$ ), PEI ( $\diamond$ )

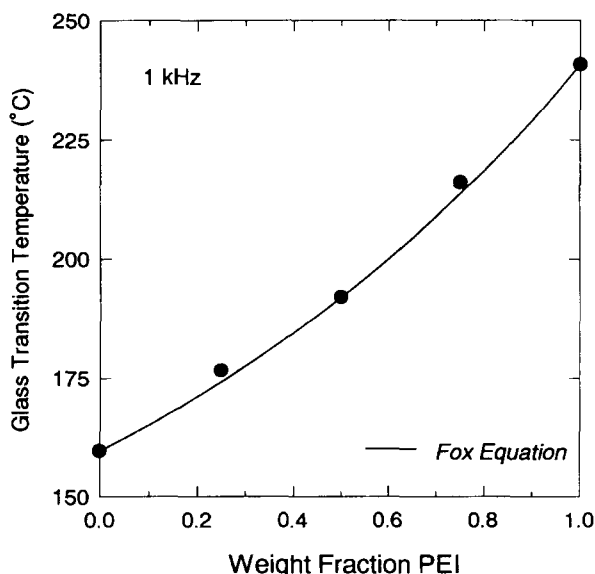


Figure 4 Dielectric glass transition temperature ( $^{\circ}\text{C}$ ) based on maximum in  $\tan \delta$  vs. weight fraction PEI for quenched amorphous blend samples. Solid line represents Fox equation<sup>5</sup>

Crystallized samples

Dielectric constant and loss factor are plotted isochronally vs. temperature for a representative melt-crystallized 50/50 PEEK/PEI blend sample in Figure 5 ( $T_{mc} = 300^{\circ}\text{C}$ ). These data reveal two successive glass-rubber relaxation events with increasing temperature which correspond to two distinct amorphous populations. A comparative plot of  $\tan \delta$  (100 kHz) vs. temperature for the constituent polymers and melt-crystallized blend samples of varying composition is provided in Figure 6; the PEEK data reported in Figure 6 correspond to PEEK 450G melt crystallized at  $300^{\circ}\text{C}$  for 1 h. Here again, each blend sample displays two relaxations. The low-temperature relaxation is significantly offset relative to that observed for melt-crystallized PEEK and displays both a systematic increase in relaxation temperature and a systematic decrease in relaxation magnitude with increasing PEI content. The position of the high-temperature relaxation

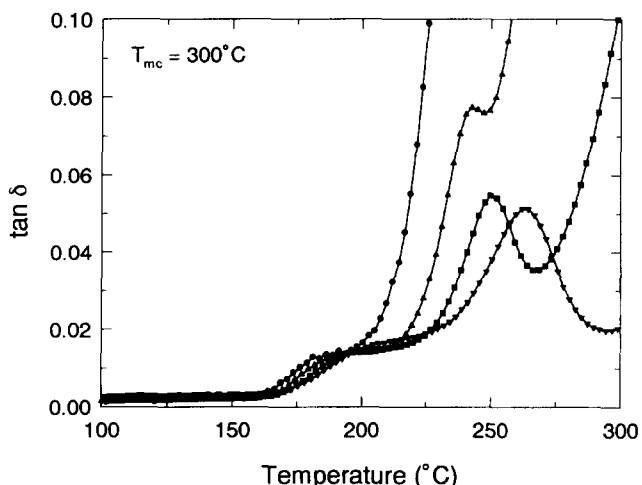
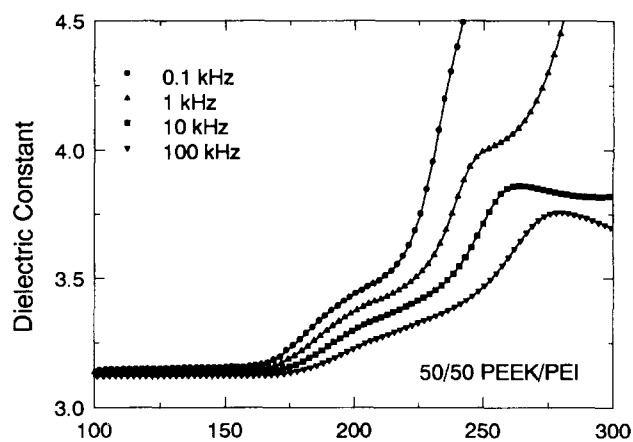


Figure 5 Dielectric constant ( $\epsilon'$ ) and loss factor ( $\tan \delta$ ) vs. temperature ( $^{\circ}\text{C}$ ) for 50/50 PEEK/PEI blend isothermally melt-crystallized at  $300^{\circ}\text{C}$ . Frequencies of 0.1 ( $\bullet$ ), 1.0 ( $\blacktriangle$ ), 10 ( $\blacksquare$ ) and 100 ( $\blacktriangledown$ ) kHz

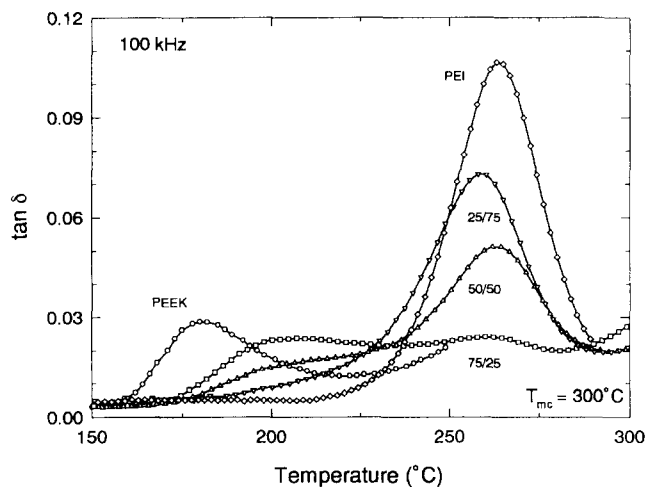


Figure 6 Dielectric  $\tan \delta$  (100 kHz) vs. temperature ( $^{\circ}\text{C}$ ) for isothermally melt-crystallized PEEK/PEI blends of varying composition ( $T_{mc} = 300^{\circ}\text{C}$ ) PEEK ( $\circ$ ), 75/25 PEEK/PEI ( $\square$ ), 50/50 PEEK/PEI ( $\Delta$ ), 25/75 PEEK/PEI ( $\nabla$ ), PEI ( $\diamond$ )

is composition invariant, and corresponds very closely to the glass transition of pure PEI. The magnitude of the high-temperature relaxation increases with increasing overall PEI content in the blend.

As noted above, SAXS measurements on crystallized PEEK/PEI blends reveal only a modest increase in the

measured lamellar long period and corresponding interlamellar spacing with increasing PEI content in the blends (low PEI concentrations), with long period independent of PEI content at higher concentrations<sup>3,4</sup>. These data suggest that relatively little PEI is retained in the interlamellar regions during crystallization. Microscopy studies<sup>6</sup> on crystallized blends of comparable thermal history show that the spherulites in these samples are space-filling; i.e. interspherulitic segregation is minimal. Taken in total, these results indicate that the high-temperature relaxation which is observed in the dielectric loss curves corresponds to an essentially pure PEI amorphous phase which is excluded between lamellar stacks and is thus primarily interfibrillar. The low-temperature relaxation corresponds to a mixed amorphous phase located between the crystal lamellae (i.e. interlamellar). The relative PEI fraction in this mixed phase increases with increasing overall PEI content, as reflected in the progressive increase in relaxation temperature.

The morphological assignments presented here for the observed amorphous phase relaxations are in agreement with those proposed previously for the PEEK/PEI blends<sup>4</sup> and are consistent with results reported for the PBT/PAR blend system<sup>16,18</sup>. The phase behaviour appears to be characteristic of crystallizable polymer blends in general when the crystallizable component has a relatively stiff backbone<sup>14</sup>. The low-temperature relaxation, while assigned here to motions originating in the interlamellar regions, may also encompass relaxation of amorphous segments in extralamellar defect regions with relatively small phase separation sizescales. However, the observation of two distinct relaxation events (as compared to a single broad relaxation), strongly suggests relaxation in two distinct morphological environments, i.e. the interlamellar mixed amorphous phase and the interfibrillar pure PEI phase.

No PEEK relaxation was evident for the blend samples, indicating the absence of a pure crystal-amorphous interphase region. This also appears to be a general result for miscible blends based on stiffer crystallizable polymers, and is consistent with penetration of the crystal-amorphous interphase by the non-crystallizable component.

#### Influence of crystallization temperature

The crystallization of PEEK results in a decrease in the conformational freedom of those PEEK chain segments held between crystal lamellae as compared to wholly-amorphous PEEK. This constraint of the amorphous PEEK segments in the crystallized blends leads to a fundamental change in the nature of intersegmental interaction between the amorphous PEEK and PEI blend components, and provides a driving force for the macroscopic exclusion of PEI from the amorphous interlamellar layer. Given this driving force, the phase-separated morphology which results as a function of composition and crystallization condition is largely dependent on kinetic factors, specifically the rate of PEI diffusion in the amorphous phase as compared to the rate of PEEK crystallization. Conditions which favour a high rate of crystallization and low PEI diffusivity will presumably lead to a higher degree of interlamellar entrapment relative to conditions which favour a low crystallization rate and higher PEI diffusivity (i.e. lower viscosity).

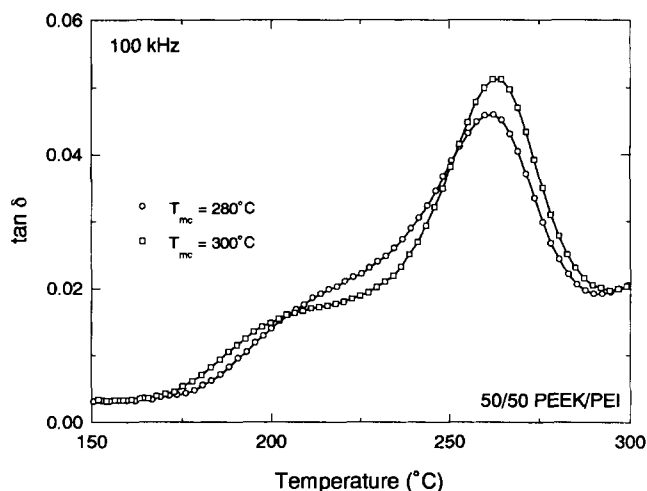


Figure 7 Dielectric  $\tan \delta$  (100 kHz) vs. temperature ( $^{\circ}\text{C}$ ) for isothermally melt-crystallized 50/50 PEEK/PEI blends.  $T_{mc} = 280^{\circ}\text{C}$  ( $\circ$ );  $T_{mc} = 300^{\circ}\text{C}$  ( $\square$ )

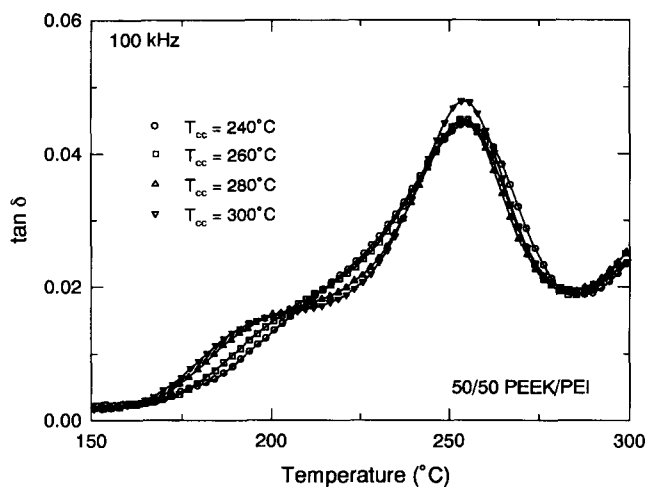
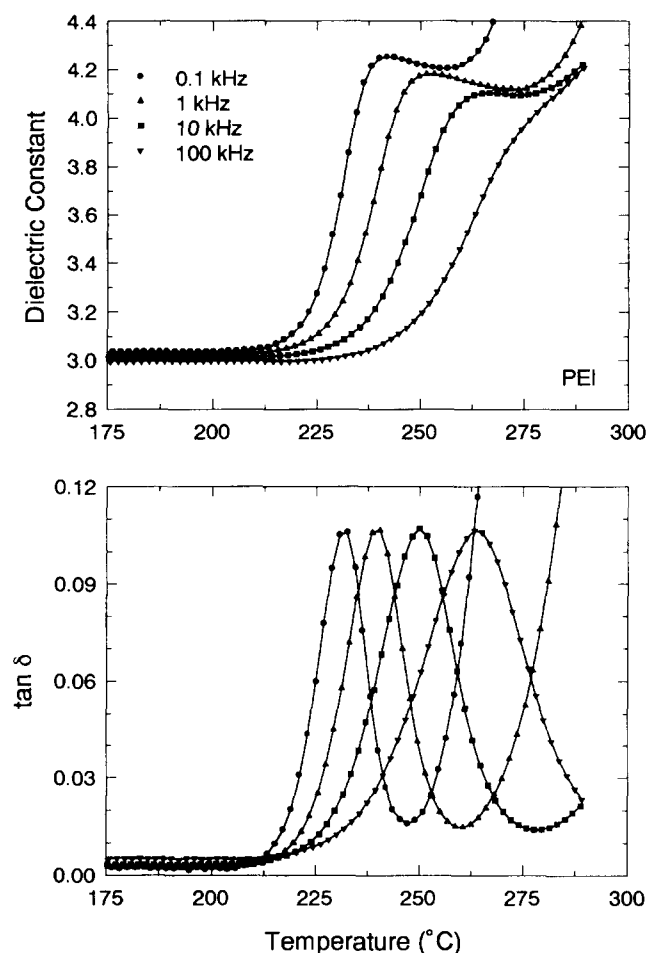


Figure 8 Dielectric  $\tan \delta$  (100 kHz) vs. temperature ( $^{\circ}\text{C}$ ) for isothermally cold-crystallized 50/50 PEEK/PEI blends.  $T_{cc} = 240^{\circ}\text{C}$  ( $\circ$ );  $T_{cc} = 260^{\circ}\text{C}$  ( $\square$ );  $T_{cc} = 280^{\circ}\text{C}$  ( $\triangle$ );  $T_{cc} = 300^{\circ}\text{C}$  ( $\nabla$ )

Comparison of  $\tan \delta$  curves for PEEK/PEI blends isothermally crystallized at varying temperature reveals trends in relaxation position and magnitude which are consistent with this scenario. In Figure 7, loss factor curves for 50/50 PEEK/PEI samples melt crystallized at 280 and 300 $^{\circ}\text{C}$  are presented. Based on the discussion of morphology development, above, an increase in interlamellar PEI content would be anticipated in the blend crystallized at 280 $^{\circ}\text{C}$ , at which temperature the PEEK crystallization rate would be increased and the PEI diffusivity decreased as compared to the 300 $^{\circ}\text{C}$  crystallization condition. (Note: kinetic studies reported by Hsiao and Sauer<sup>3</sup> indicate a maximum in the crystallization rate for 50/50 PEEK/PEI at  $\sim 260^{\circ}\text{C}$ .) This result is observed in Figure 7. The low-temperature (interlamellar) relaxation displays a stronger relaxation intensity in the 280 $^{\circ}\text{C}$  sample, with the relaxation offset to a higher temperature indicating a greater PEI fraction in the mixed amorphous phase. Examination of the high-temperature (interfibrillar/interspherulitic) loss peak reveals a higher relaxation magnitude for the sample crystallized at 300 $^{\circ}\text{C}$ , again in agreement with the



**Figure 9** Dielectric constant ( $\epsilon'$ ) and loss factor ( $\tan \delta$ ) vs. temperature ( $^{\circ}\text{C}$ ) for Ultem 1000 PEI. Frequencies of 0.1 (●), 1.0 (▲), 10 (■) and 100 (▼) kHz.

scenario described above. Comparison of  $\tan \delta$  curves for a series of cold-crystallized 50/50 PEEK/PEI samples shows the same trend, with the level of interlamellar PEI entrapment progressively increasing with decreasing cold crystallization temperature (Figure 8). In all cases, however, the coexistence of both an interlamellar mixed phase and a pure PEI phase is clearly indicated.

*PEI glass-rubber relaxation*

One of the advantages of dielectric relaxation spectroscopy for the study of crystallizable blends is the information it provides as to the composition of the various amorphous populations as reflected in their observed relaxation temperatures. The application of an appropriate mixing rule (e.g. the Fox equation) in conjunction with knowledge of the pure component relaxation temperatures allows for direct determination of the composition of the individual amorphous phases. In the case of the crystallized PEEK/PEI blend samples, there is a sizeable degree of overlap between the two observed amorphous phase relaxations, and this renders determination of the individual relaxation peak temperatures somewhat problematic.

We have adopted a phenomenological data fitting approach in an effort to separate the two amorphous phase relaxations, and thereby establish the individual relaxation temperatures in an unambiguous manner. In order to describe the high-temperature (interfibrillar/ interspherulitic) relaxation in the crystallized blends, it is appropriate to first consider the relaxation characteristics of pure PEI. Dielectric constant and loss factor are plotted vs. temperature for Ultem 1000 in the vicinity of the glass-rubber relaxation in Figure 9. The step-wise increase in  $\epsilon'$  and sharp maximum in  $\tan \delta$  are characteristic of the glass transition in amorphous materials. The strong increase in loss factor at lower frequencies/higher temperatures corresponds to the onset of conduction: the influence of conduction was

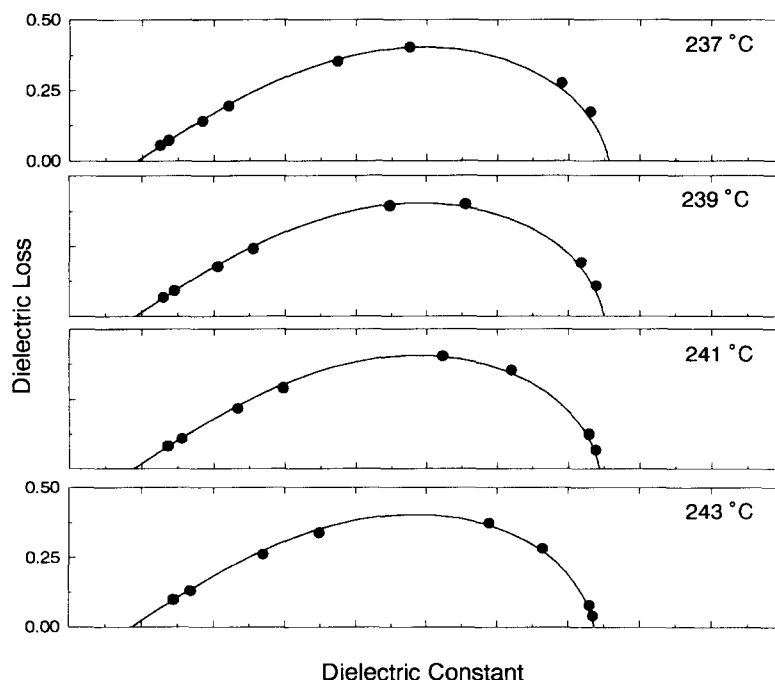


**Figure 10** Argand diagrams for PEI in the vicinity of the glass-rubber relaxation. Solid curves represent best fits to the Havriliak-Negami equation

removed from the dielectric loss data in the region of the glass transition prior to analysis by methods described previously<sup>21</sup>.

Dielectric data for pure PEI were analysed using the Havriliak–Negami modification of the single relaxation time Debye expression<sup>22</sup>.

$$\varepsilon^* = \varepsilon_U + \frac{(\varepsilon_R - \varepsilon_U)}{[1 + (i\omega\tau)^\beta]^\alpha} \quad (1)$$

where  $\varepsilon_R$  and  $\varepsilon_U$  represent the relaxed ( $\omega \rightarrow 0$ ) and the unrelaxed ( $\omega \rightarrow \infty$ ) values of the dielectric constant,  $\omega$  is the frequency,  $\tau$  is the central relaxation time, and  $\beta$  and  $\alpha$  are the broadening and skewing parameters, respectively. When  $\beta = 1$ , equation (1) reduces to the Davidson–Cole<sup>23</sup> expression corresponding to a dispersion in the shape of a skewed semicircle, while for  $\alpha = 1$ , a symmetric arc results (Cole–Cole form<sup>24</sup>). When both  $\beta$  and  $\alpha$  are equal to unity, the Debye expression is recovered. Argand diagrams plotting dielectric loss ( $\varepsilon'' = \varepsilon' \tan \delta$ ) vs. dielectric constant were constructed at selected temperatures in the vicinity of the glass transition (Figure 10). The five parameters inherent to equation (1) [ $\varepsilon_R$ ,  $\varepsilon_U$ ,  $\tau$ ,  $\beta$ ,  $\alpha$ ] were determined at each temperature of interest by a least-squares curve fitting approach, with initial parameter values estimated using the method outlined in ref. 22. The temperature-dependence of these parameters was expressed in a manner similar to the method presented by Coburn and Boyd for the glass–rubber relaxation in PET<sup>25</sup>, wherein  $\varepsilon_R$ ,  $\varepsilon_U$ , and  $\beta$  are linear functions of temperature,  $\alpha$  is independent of temperature, and  $\tau$  is described by the WLF equation<sup>26</sup>. The results for PEI are as follows:

$$\varepsilon_R = 5.87 - 0.0066T(^{\circ}\text{C}) \quad (2a)$$

$$\varepsilon_U = 3.53 - 0.0023T(^{\circ}\text{C}) \quad (2b)$$

$$\beta = 0.61 + 0.0012T(^{\circ}\text{C}) \quad (2c)$$

$$\alpha = 0.487 \quad (2d)$$

$$\log_{10} \left( \frac{\tau}{\tau_0} \right) = \frac{-11.20(T - T_0)}{58.93 + (T - T_0)} \quad (2e)$$

$(\tau_0 = 1\text{ s}; \quad T_0 = 221.5^{\circ}\text{C})$

The corresponding isochronal dielectric constant and loss curves based on these expressions are plotted vs. temperature in Figure 11; good agreement with the experimental data is achieved.

#### Crystallized blend curve fits and phase compositions

The dielectric loss curves for the crystallized PEEK/PEI blends were empirically fit using a procedure based on the combination of two independent relaxations. The low-temperature relaxation was fit using the Cole–Cole form of equation (1) (i.e. no skewing), which is consistent with the shape of the dispersion observed for crystallized PEEK<sup>19</sup>. The high-temperature relaxation was fit using the temperature-dependent Havriliak–Negami form as described above. While the dielectric strength and broadening/skewing parameters were allowed to scale freely in order to fit the blend data, the time–temperature (WLF) parameters used in the (high-temperature) blend fits were essentially the same as those obtained for pure PEI.

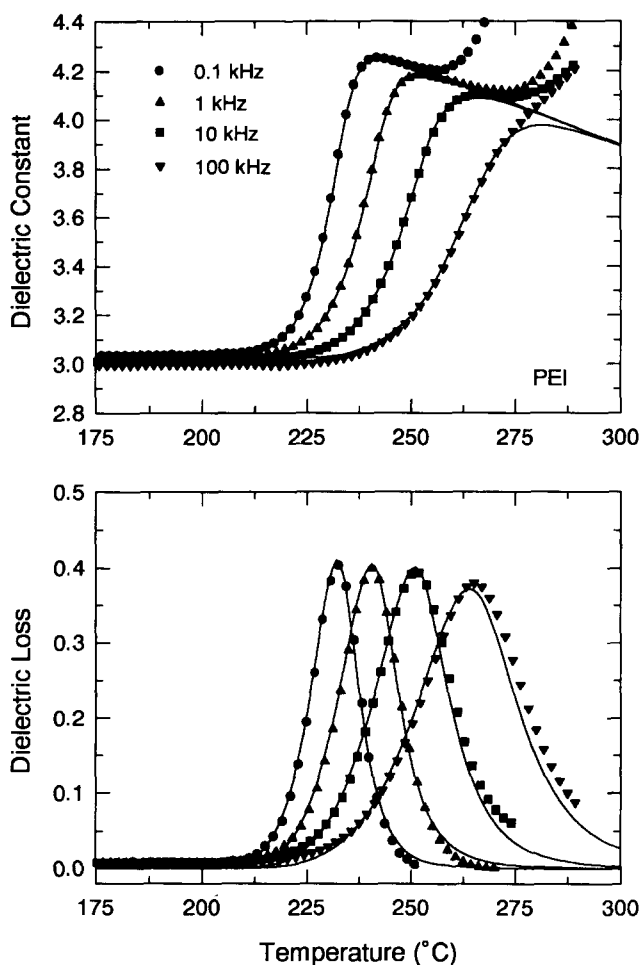


**Figure 11** Dielectric constant ( $\varepsilon'$ ) and conduction-corrected dielectric loss ( $\varepsilon''$ ) vs. temperature ( $^{\circ}\text{C}$ ) for PEI. Solid curves represent temperature-dependent Havriliak–Negami best fits according to equations (2)

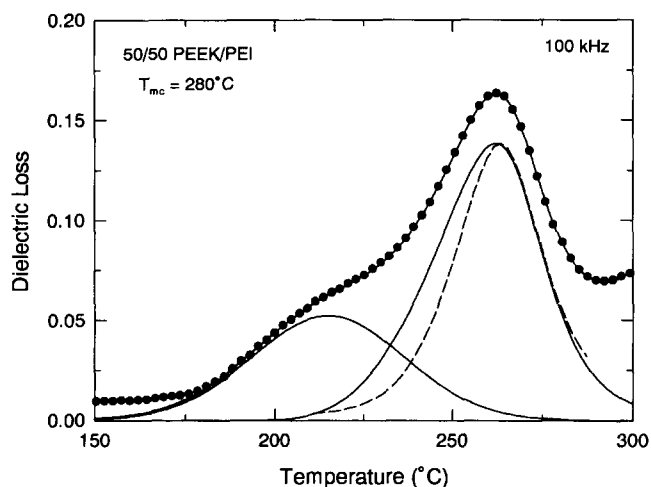


**Figure 12** Dielectric loss (100 kHz) vs. temperature ( $^{\circ}\text{C}$ ) for 50/50 PEEK/PEI blend melt-crystallized at  $280^{\circ}\text{C}$ . Best-fit curve (through data) represents sum of low-temperature Cole–Cole fit (*interlamellar* component) and high-temperature Havriliak–Negami fit (*interfibrillar/ interspherulitic* component), plus conduction correction (not shown). Dashed curve represents relaxation for pure PEI

Dielectric loss results for the 50/50 PEEK/PEI blend composition melt crystallized at  $280^{\circ}\text{C}$  are shown by way of example in Figure 12. The  $\varepsilon''$  vs. temperature data have been resolved into two overlapping relaxations,

demonstrating the validity of the empirical method for the resolution of the individual relaxation temperatures. This approach is most effective for the highest test frequency examined (100 kHz), as the influence of conduction is minimal.

The dashed line included in *Figure 12* corresponds to the glass–rubber relaxation in pure PEI; the magnitude of the pure PEI relaxation has been scaled to match the magnitude of the high-temperature blend relaxation. It is evident that the interfibrillar/interspherulitic relaxation in the crystallized blend is broader than that observed for pure PEI, despite the coincidence of their relaxation temperatures. The low-temperature broadening reflects the fact that the PEI in the crystallized blend experiences a spectrum of local relaxation environments ranging continuously from the nanometre sizescale (interlamellar environment) to the micrometre sizescale (interfibrillar/interspherulitic environment).

The relaxation temperatures of the individual amorphous phases in the crystallized PEEK/PEI blends were established for the various compositions and crystallization conditions using the dual curve fitting approach described above; all temperatures were determined for a test frequency of 100 kHz. These results are plotted as relaxation temperature vs. crystallization temperature in *Figure 13*. As was indicated previously, the high-temperature (interfibrillar/interspherulitic) relaxation in the blends corresponds very closely to a pure PEI glass transition for all sample histories. The low-temperature (interlamellar) relaxation is shifted to higher temperatures with increasing overall PEI content in the blend. For the cold-crystallized samples, the interlamellar relaxation temperature decreases with increasing crystallization temperature, which indicates less interlamellar trapping at less restrictive crystallization conditions. This effect is less pronounced over the limited range of melt crystallization temperatures.

The composition of the individual amorphous phases in the blends can be estimated by the application of the Fox equation using the approach described by Runt *et al.*<sup>18</sup> (see also Cebe<sup>16</sup>). One complication, however, is the determination of the pure component glass transitions. Specifically, the glass transition temperature of crystallized PEEK is sensitive to the degree of constraint imposed on the amorphous segment motions by the crystalline morphology. More restrictive crystallization conditions lead to a greater degree of motional constraint and a correspondingly higher relaxation temperature, while less restrictive crystallization conditions produce less constraint and a lower relaxation temperature. This effect is shown in *Figure 13a*, where the relaxation temperature of cold-crystallized PEEK decreases with increasing crystallization temperature. The issue is further complicated in that the Fox equation requires a pure component transition temperature which reflects the transition characteristics of the amorphous PEEK chains within the blend specimen morphology, i.e. in the presence of PEI. The presence of PEI in the blends has a significant effect on the lamellar morphology which develops and the corresponding constraint which is imposed on the relaxing PEEK segments. For the purposes of estimating amorphous phase compositions in this work, the pure PEEK relaxation temperatures used in the Fox equation were those corresponding to semicrystalline PEEK specimens prepared at the same crystallization conditions.

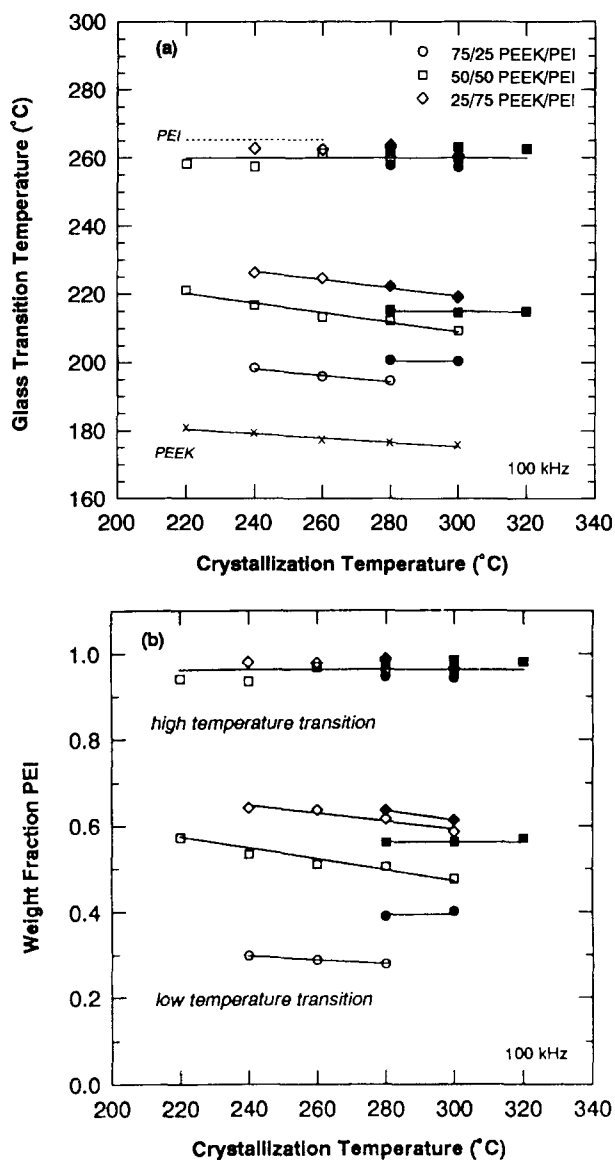


**Figure 13** Relaxation characteristics of thermally-crystallized PEEK/PEI blends as a function of crystallization temperature. (a) Glass transition temperature (°C) vs. crystallization temperature. (b) Weight fraction PEI vs. crystallization temperature (°C) according to the Fox equation. 75/25 PEEK/PEI (○), 50/50 PEEK/PEI (□), 25/75 PEEK/PEI (◇). Open symbols: cold crystallization. Filled symbols: melt crystallization. Cold-crystallized PEEK results (×) from ref. 19

The phase compositions for the two amorphous populations in the crystallized blends are plotted against crystallization temperature in *Figure 13b*. The trends in phase composition as a function of overall blend ratio and crystallization temperature are consistent with the discussions, above. Examination of the low-temperature (interlamellar) phase composition as a function of initial blend composition indicates values which are comparable to those calculated by Runt *et al.* for PBT/PAR<sup>18</sup>, and which are consistent with the scans reported by Jonas *et al.*<sup>4</sup> for PEEK/PEI. In both of those studies, a plateau value in interlamellar composition was reported at levels of 50% and greater noncrystallizable component in the blend. This was consistent with the corresponding SAXS data, which showed no variation in long spacing across this composition range. For the data reported here, the variation in interlamellar composition with blend ratio observed at high overall



PEI content must be interpreted cautiously, owing to the degree of uncertainty inherent in separating the overlapping dielectric relaxations for the 25/75 PEEK/PEI scans. Also, it should be noted that based on the Fox equation, the observed trend in the low-temperature glass transition with crystallization temperature does reflect a tangible change in the composition of the mixed phase held in the interlamellar regions, and is not simply a manifestation of crystalline constraint effects as are observed for pure PEEK.

## CONCLUSIONS

A series of detailed dielectric studies have been performed for PEI and PEEK/PEI blends of varying composition as a function of crystallization condition. Quenched amorphous blend samples displayed a single glass transition which shifted with composition according to the Fox equation. Thermally-crystallized specimens displayed the coexistence of two amorphous phase populations at all blend ratios corresponding to a mixed phase held between the crystal lamellae and a pure PEI phase located in interfibrillar and interspherulitic regions. No PEEK relaxation was observed, indicating the absence of a pure crystal-amorphous interphase. The overlapping peaks in dielectric loss were resolved into their constituent relaxations using a dual curve fit procedure whereby the low-temperature (interlamellar) relaxation was described by a temperature-dependent Cole-Cole form, while the high-temperature (interfibrillar/interspherulitic) relaxation was described by the Havriliak-Negami equation, consistent with results obtained for pure PEI. The composition of the interlamellar phase was enriched in PEI with increasing overall PEI content in the blend. Lower crystallization temperatures led to an increase in the amount of PEI trapped in the interlamellar regions, which was consistent with kinetic control of the evolving morphology: as crystallization temperature decreased, the crystallization rate increased and PEI diffusivity decreased, thus leading to greater interlamellar entrapment. Comparison of the high-temperature (interfibrillar/interspherulitic) relaxation with that of pure PEI showed that the PEI relaxation in the crystallized blends was broadened as compared to the amorphous homopolymer, indicating that the PEI in the blends

experiences a wide spectrum of local relaxation environments across a range of sizescales.

## ACKNOWLEDGEMENTS

This work was supported in part by a graduate research assistantship from the US Department of Education (Grant P200A10166 to J.F.B.). We are pleased to acknowledge Dr Ron Greenberg at GE Plastics for supplying the Ultem PEI resin.

## REFERENCES

- Harris, J. E. and Robeson, L. M. *J. Appl. Polym. Sci.* 1988, **35**, 1877
- Crevecoeur, G. and Groeninckx, G. *Macromolecules* 1990, **24**, 1190
- Hsiao, B. S. and Sauer, B. B. *J. Polym. Sci., Polym. Phys. Ed.* 1993, **32**, 901
- Jonas, A. M., Russell, T. P. and Yoon, D. Y. *Proc. Am. Chem. Soc. Div. Polym. Mater. Sci. Eng.* 1994 **70**, 394
- Fox, T. G. *Bull. Am. Phys. Soc.* 1956, **1**, 123
- Hudson, S. D., Davis, D. D. and Lovinger, A. J. *Macromolecules* 1992, **25**, 1759.
- Hahn, B., Wendorff, J. and Yoon, D. *Macromolecules* 1985, **18**, 718
- Hahn, B. R., Herrmann-Schönherr, O. and Wendorff, J. H. *Polymer* 1987, **28**, 201
- Ando, Y. and Yoon, D. Y. *Polym. J.* 1992, **24**, 1329
- Alfonso, G. C. and Russell, T. P. *Macromolecules* 1986, **19**, 1143
- Russell, T. P., Ito, H. and Wignall, G. D. *Macromolecules* 1988, **21**, 1703
- Kumar, S. K. and Yoon, D. Y. *Macromolecules* 1989, **22**, 4098
- Kumar, S. K. and Yoon, D. Y. *Macromolecules* 1991, **24**, 5414
- Runt, J. P., Barron, C. A., Zhang, X. and Kumar, S. *Macromolecules* 1991, **24**, 3466
- Huo, P. P. and Cebe, P. *Macromolecules* 1993, **26**, 3127
- Huo, P. P., Cebe, P. and Capel, M. *Macromolecules* 1993, **26**, 4275
- Runt, J. P., Miley, D. M., Zhang, X., Gallagher, K. P., McFeaters, K. and Fishburn, J. *Macromolecules* 1992, **25**, 1929
- Runt, J. P., Zhang, X., Miley, D. M., Gallagher, K. P. and Zhang, A. *Macromolecules* 1992, **25**, 3902
- Kalika, D. S. and Krishnaswamy, R. K. *Macromolecules* 1993 **26**, 4252
- Krishnaswamy, R. K. and Kalika, D. S. *Polymer* 1994, **35**, 1157
- Kalika, D. S. and Yoon, D. Y. *Macromolecules* 1991 **24**, 3404
- Havriliak, S. and Negami, S. *J. Polym. Sci. Part C* 1996, **14**, 99
- Davidson, D. W. and Cole, R. H. *J. Chem. Phys.* 1950, **18**, 1417
- Cole, R. H. and Cole, K. S. *J. Chem. Phys.* 1941, **9**, 341
- Coburn, J. C. and Boyd, R. H. *Macromolecules* 1986, **19**, 2238
- Ferry, J. D. 'Viscoelastic Properties of Polymers', Wiley, New York, 1980